Pramana – J. Phys. (2019) 92:6
https://doi.org/10.1007/s12043-018-1672-4

Decay of $Z = 82-102$ heavy nuclei via emission of one-proton and two-proton halo nuclei

K P SANTHOSH* and INDU SUKUMARAN

School of Pure and Applied Physics, Kannur University, Swami Anandatheertha Campus, Payyanur 670 327, India
*Corresponding author. E-mail: drkpsanthosh@gmail.com

MS received 13 January 2018; revised 30 May 2018; accepted 4 June 2018; published online 30 October 2018

Abstract. The halo structure of a nucleus is investigated on the basis of separation energy consideration and potential energy calculations. Most of the predictions on the existence of halo nuclei are found to agree with the available experimental studies. For the first time, the possibility of emitting proton halo (p-halo) nuclei from heavy nuclei within the range $82 \le Z \le 102$ has been studied by evaluating decay half-lives for the emission of 1p-halo nuclei ^{8}B, ^{12}N, ^{13}N, ^{17}F and 2p-halo nuclei ^{9}C, ^{17}Ne, ^{18}Ne, ^{20}Mg using Coulomb and proximity potential model (CPPM). Of these, the emissions of 1p-halo nuclei ^{8}B, ^{12}N, ^{13}N and ^{17}F are found to be probable from various heavy nuclei as the half-lives of the corresponding emissions are within the experimental upper limit ($T_{1/2} \le 10^{30}$ s). When dealing with 2p-halo nuclei, its emission is observed to be less probable compared to 1p-halo nuclei, except ^{18}Ne. Compared to the probability of emission of a normal cluster, the probability of emission of a p-halo nucleus from a radioactive nuclide is found to be less but still, there is a finite probability of p-halo emissions from heavy nuclei.

Keywords. Heavy particle decay; halo nuclei; α-decay.

PACS Nos **23.70.+j; 23.60.+e; 27.90.+b**

1. Introduction

The existence of exotic nuclei has become the focus of interest due to the unusual phenomena exhibited by them. In the region of the driplines, the structural changes of the nuclei lead to dramatic nuclear behaviour such as a nuclear halo, a new paradigm in physics at the driplines. The nuclear halo state is observed to be resulting from the weak binding of the valence nucleons and the separation of the valence nucleons, most probably neutrons, from the inert core containing all other nucleons [1–4]. The credit of the discovery of halo nuclei goes to Tanihata *et al* [5,6], in 1985, and this was confirmed later by Hansen and Jonson [7].

For obtaining a deep insight into the halo nuclei, radioactive beam facilities are widely used [8–11]. ^{6}He was the first halo nucleus produced in the laboratory and it belongs to a neutron halo nucleus [12]. The other experimentally confirmed halo nuclei are ^{11}Li, ^{11}Be, ^{14}Be, ^{14}B, ^{15}C and ^{19}C [13], all belonging to neutron halo systems. Several other proposals for neutron halo nuclei awaiting more experimental confirmation include ^{15}B, ^{17}B [14], ^{19}B, ^{22}C and ^{23}O [2]. The key evidence to obtain information on the existence of halo nuclei is the reaction cross-section measurements [5,6]. Tanaka *et al* [15], initiating a nuclear reaction using ^{22}C on a liquid hydrogen in search of a halo nucleus, noticed a high value of cross-section around 40 A MeV compared to the values obtained for other adjacent carbon nuclei. There exists an updating report supporting the halo character of ^{22}C from the interaction cross-section measurements carried out by Togano *et al* [16]. Recently, Takechi *et al* [17] and Kobayashi *et al* [18] confirmed that ^{37}Mg is a p-wave neutron halo nucleus and is the heaviest deformed halo candidate. The cross-section studies of ^{17}F [19], ^{11}Be [20,21], ^{6}He [22–27], ^{9,11}Li [28–31] and other neutron halo projectile studies [7,9,32–34] also are of great significance.

To explain what constitutes a halo nucleus and under what conditions it will manifest itself, several structure models and reaction models are available. The structure models include two-body systems, three-body systems [35] and microscopic models [36,37]. In addition, the reaction models [2,38–41] have also been used to describe features of halo nuclei.

The proton halo (p-halo) nuclei are less pronounced compared to neutron halo nuclei [2,7]. However, examples include ^{8}B, ^{12}N, ^{13}N and ^{17}F (1p-halo nuclei) and ^{9}C, ^{17}Ne, ^{18}Ne and ^{20}Mg (2p-halo nuclei) [42–48]. Among the various p-halo candidates suggested, the 1p-halo structures are established for ^{8}B [44,49,50] and ^{17}F [51,52] and the 2p-halo for only ^{17}Ne [51]. Besides the above proposed p-halo nuclei, ^{26}P, ^{27}P, ^{23}Al [53] and ^{27}S are some other suggested candidates of p-halo nuclei [54,55].

The fusion studies carried out for the p-halo systems have shown the existence of increased fusion cross-section, thereby the fusion enhancement. Even though the fusion studies are presently less, the fusion data are available for the 1p-halo systems, ^{8}B + ^{58}Ni [56,57], ^{8}B +^{28}Si [58] and ^{8}B +^{12}C [59]. Several other cross-section studies have also been conducted for the p-halo systems [57,60–63]. All these fusion studies, both experimental and theoretical, motivated us to think about the reverse process involving halo systems. With this intention, in the present paper, we focussed on the heavy particle radioactivity (HPR) [64,65] of heavy nuclei emitting p-halo nuclei using the Coulomb and proximity potential model (CPPM) which has been used as a powerful tool in the HPR studies [66–69].

In the present work, we analysed the halo structure of a nucleus on the basis of potential energy consideration and separation energy calculations, thereby characterising a nucleus as a halo nucleus. Further, we emphasised the possibility of emitting p-halo nuclei from various heavy nuclei parents ranging from $Z = 82$ to 102 by calculating the decay half-lives for the emission of 1p-halo nuclei ^{8}B, ^{12}N, ^{13}N, ^{17}F and 2p-halo nuclei ^{9}C, ^{17}Ne, ^{18}Ne, ^{20}Mg.

The details of the model are described in §2. In §3 the results of our calculations are given and in §4 major conclusions of the study are presented.

2. The CPPM

In CPPM [70,71], the potential energy barrier is taken as the sum of Coulomb potential, proximity potential and centrifugal potential for the touching configuration and for separated fragments. For the pre-scission (overlap) region, the interacting potential barrier is obtained using the simple power law interpolation method as done by Shi and Swiatecki [72]. The interacting potential barrier for a parent nucleus exhibiting cluster decay is given by

$$V = \frac{Z_1 Z_2 e^2}{r} + V_{\mathrm{p}}(z) + \frac{\hbar^2 \ell(\ell+1)}{2\mu r^2}, \quad \text{for } z > 0. \tag{1}$$

Here Z_1 and Z_2 are the atomic numbers of the daughter and emitted clusters, respectively, z is the distance between the near surfaces of the fragments, r is the distance between fragment centres and is given as $r = z + C_1 + C_2$, where C_1 and C_2 are the Süsmann central radii of fragments. The term ℓ represents the angular momentum, μ is the reduced mass and V_{p} is the proximity potential. The proximity potential V_{p} is given by Blocki *et al* [73] and Blocki and Swiatecki [74] as

$$V_{\mathrm{p}}(z) = 4\pi\gamma b \left[\frac{C_1 C_2}{(C_1 + C_2)}\right] \Phi\left(\frac{z}{b}\right) \tag{2}$$

with the nuclear surface tension coefficient

$$\gamma = 0.9517[1 - 1.7826(N-Z)^2/A^2]\,\mathrm{MeV/fm^2}, \tag{3}$$

where N, Z and A represent the neutron, proton and mass number of parents, respectively,Φ represents the universal proximity potential [74] given as

$$\Phi(\varepsilon) = -4.41\mathrm{e}^{-\varepsilon/0.7176}, \quad \text{for } \varepsilon > 1.9475, \tag{4}$$

$$\Phi(\varepsilon) = -1.7817 + 0.9270\varepsilon + 0.01696\varepsilon^2 - 0.05148\varepsilon^3, \quad \text{for } 0 \le \varepsilon \le 1.9475 \tag{5}$$

with $\varepsilon = z/b$, where the width (diffuseness) of the nuclear surface $b \approx 1$ fm and Süsmann central radii C_i of the fragments related to sharp radii R_i is

$$C_i = R_i - \left(\frac{b^2}{R_i}\right). \tag{6}$$

For R_i we use the semi-empirical formula in terms of mass number A_i as [74]

$$R_i = 1.28A_i^{1/3} - 0.76 + 0.8A_i^{-1/3}. \tag{7}$$

The potential for the internal part (overlap region) of the barrier is given as

$$V = a_0(L - L_0)^n, \quad \text{for } z < 0. \tag{8}$$

Here $L = z + 2C_1 + 2C_2$ and $L_0 = 2C$, the diameter of the parent nuclei. The constants a_0 and n are determined by the smooth matching of the two potentials at the touching point.

The barrier penetrability P is given as

$$P = \exp\left\{-\frac{2}{\hbar}\int_a^b \sqrt{2\mu(V-Q)}\,\mathrm{d}z\right\}. \tag{9}$$

Here the mass parameter is replaced by $\mu = mA_1A_2/A$, where m is the nucleon mass and A_1, A_2 are the mass numbers of the daughter and the emitted clusters, respectively. The inner and outer turning points a and b are defined as $V(a) = V(b) = Q$, where Q is the energy released. The half lifetime is given by

$$T_{1/2} = \left(\frac{\ln 2}{\lambda}\right) = \left(\frac{\ln 2}{\nu P}\right), \tag{10}$$

Here, $P = SP_s$, S is the pre-formation probability calculated as the penetrability of the internal part of the

Table 1. The calculated halo characteristics of light proton-rich nuclei. The 1p and 2p separation energies are calculated by using the mass excess tables of Wang *et al* [77].

Structure	Nucleus	$S(p)$ (keV)	$S(2p)$ (keV)	Cluster + core configuration
1p-halo	^{8}B	136.371	5743.220	1p+^{7}Be
	^{12}N	601.171	9290.541	1p+^{11}C
	^{13}N	1943.491	17900.361	1p+^{12}C
	^{17}F	600.269	12727.680	1p+^{16}O
2p-halo	^{9}C	1299.571	1435.941	2p+^{7}Be
	^{17}Ne	1468.471	933.041	2p+^{15}O
	^{18}Ne	3923.071	4523.340	2p+^{16}O
	^{20}Mg	2658.971	2336.541	2p+^{18}Ne

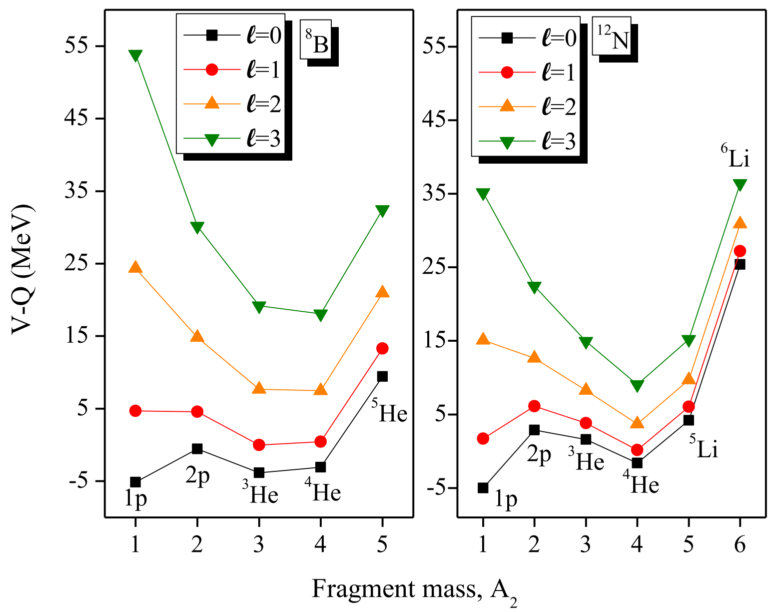

Figure 1. The driving potential $V–Q$ as a function of the light cluster mass A_2 for 1p-halo nuclei, ^{8}B and ^{12}N, showing the deepest minimum at 1p-cluster + core configurations.

barrier, P_s is the quantum penetrability of the external potential barrier, $\nu = (\omega/2\pi) = (2E_v/h)$ represents the number of assaults on the barrier per second and λ is the decay constant. The empirical vibration energy, E_v, is given as [75]

$$E_v = Q\left\{0.056 + 0.039\exp\left[\frac{(4-A_2)}{2.5}\right]\right\},\quad \text{for } A_2 \geq 4. \tag{11}$$

3. Results and discussion

In the field of halo nucleus, major studies were concentrated on neutron halo nuclei. Although the formation of p-halo nuclei becomes possible at the proton driplines, it is less developed compared to neutron halo nuclei. So, the p-halo candidates are still awaiting more theoretical and experimental confirmations. In this context, we have performed an extensive study on p-halo structure of a nucleus and its existence in proton dripline via heavy particle decay studies, for the first time.

It may be mentioned that in order to characterise a nucleus as a p-halo nucleus, the major tools used are the separation energy consideration and potential energy calculations with which one can obtain the halo structure of a nucleus. A major tool to identify the p-halo structure of a nucleus is to measure its low proton separation energy. The $1p$ and $2p$ separation energies [76] are defined in terms of mass excesses as

$$S(p) = -\Delta M(A, Z) + \Delta M(A-1, Z-1) + \Delta M_H = -Q(\gamma, p), \tag{12}$$

$$S(2p) = -\Delta M(A, Z) + \Delta M(A-2, Z-2) + 2\Delta M_H = -Q(\gamma, 2p), \tag{13}$$

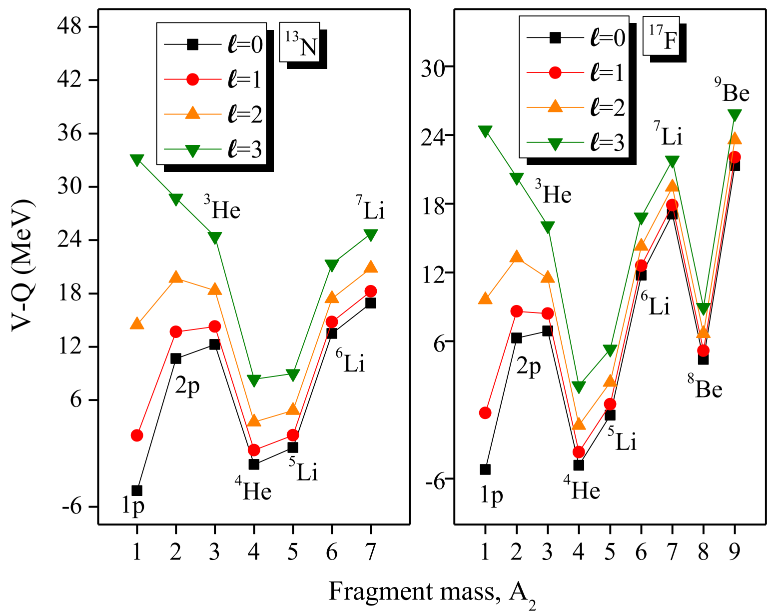

Figure 2. The driving potential V–Q as a function of the light cluster mass A_2 for 1p-halo nuclei, ^{13}N and ^{17}F, showing the deepest minimum at 1p-cluster + core configurations.

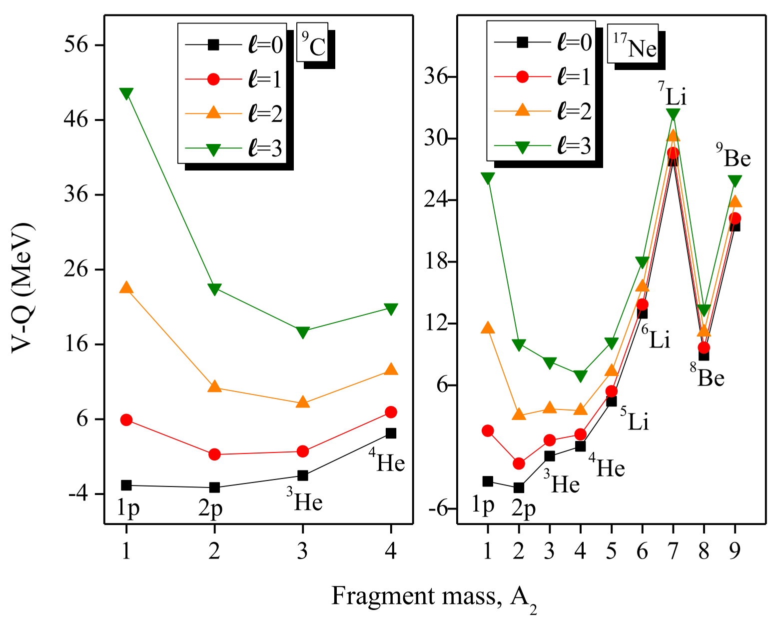

Figure 3. The driving potential V–Q as a function of the light cluster mass A_2 for 2p-halo nuclei, ^{9}C and ^{17}Ne.

where $S(p)$ and $S(2p)$ are the $1p$ and $2p$ separation energies of the nucleus, respectively, $\Delta M(A, Z)$, ΔM_H, $\Delta M(A-1, Z-1)$ and $\Delta M(A-2, Z-2)$ represent the mass excess of the parent nuclei, the mass excess of the proton, the mass excess of the daughter nuclei produced during one-proton radioactivity and the mass excess of the daughter nuclei produced during two-proton radioactivity. $Q(\gamma, p)$ and $Q(\gamma, 2p)$ represent the Q values for one-proton and two-proton radioactivity, respectively. For the separation energy evaluation, the mass excess values are taken from Wang *et al* [77].

According to the separation energy consideration, a nucleus is considered to be a 1p-halo nucleus if $S(p)$ is the lowest and 2p-halo nucleus if $S(2p)$ is the lowest, both less than 1 MeV. We have calculated $S(p)$ and $S(2p)$ for the proposed p-halo nuclei ^{8}B, ^{9}C, ^{12}N, ^{13}N, ^{17}F, ^{17}Ne, ^{18}Ne and ^{20}Mg. In table 1, we have listed all

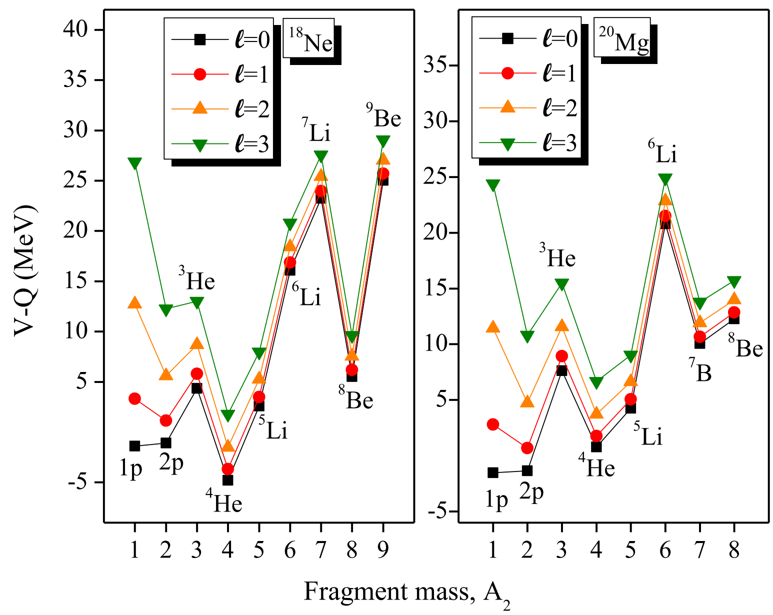

Figure 4. The driving potential V–Q as a function of the light cluster mass A_2 for 2p-halo nuclei, ^{18}Ne and ^{20}Mg.

the cases of p-halo nuclei studied in the present paper with their proton separation energies $S(p)$ and $S(2p)$. Of these, it is to be noticed that the nuclei ^{8}B, ^{12}N, ^{13}N and ^{17}F show 1p separation energy, $S(p)$, as the lowest and these candidates can be considered as 1p-halo nuclei, whereas in the case of ^{17}Ne and ^{20}Mg, $S(2p)$ is the lowest and they are considered as 2p-halo nuclei as per the separation energy consideration. However, in table 1, we notice a disagreement with the separation energy consideration that ^{9}C and ^{18}Ne were proposed to be 2p-halo nuclei but were not obtained as expected since $S(2p)$ is higher than $S(p)$ and both values are larger than ∼1 MeV. For ^{18}Ne and ^{20}Mg, both the separation energies are much larger than 1 MeV, which may be the case of collective soft dipole excitations [78].

We have calculated the driving potential (V–Q) for touching configuration ($z = 0$) for all the p-halo nuclei listed in table 1. To calculate the driving potential (V–Q), the mass excess values are taken from Wang *et al* [77]. For a particular p-halo candidate, (V–Q) is obtained for all its possible cluster–core configurations. Here the term cluster is used as a general term for 1p, 2p, α-particle and heavier nuclei. We look for a cluster–core configuration with minimum (V–Q), which means that the quantum mechanical probability is larger for that particular configuration. The results of our calculations for the 1p-halo and 2p-halo structures are given in figures 1–4. In order to consider the angular momentum part of the potential, we have included calculations for $\ell = 0, 1, 2, 3$, chosen arbitrarily. Figure 1 shows the driving potential V–Q against A_2 (cluster mass) plot for the 1p-halo nuclei, ^{8}B, ^{12}N, and figure 2 shows the same for ^{13}N and ^{17}F. The figures show that in all the cases the deepest minimum is obtained for 1p+core configuration (for $\ell = 0$), consistent with the separation energy calculations presented in table 1. For higher values of angular momentum, a shift is observed in the minimum to another cluster which needs further investigation and it may be due to the mixed angular momentum and parity states of the ground-state configuration [30]. Figure 3 shows the potential energy calculations of 2p-halo nuclei ^{9}C, ^{17}Ne and figure 4 shows the same for ^{18}Ne and ^{20}Mg. For ^{9}C and ^{17}Ne (figure 3), the minimum corresponds to 2p+core configuration which confirmed its 2p-halo structure. Regarding the halo nuclei ^{18}Ne and ^{20}Mg, we have seen some discrepancies in the position of minimum. However, the calculations have shown a general trend of minimum potential energy at 2p+core configurations.

This paper aims to check whether any p-halo nucleus would be emitted from heavy nuclei, thereby helps in confirming the existence of p-halo candidates. We have studied the probable emissions of p-halo nuclei ^{8}B, ^{9}C, ^{12}N, ^{13}N, ^{17}F, ^{17}Ne, ^{18}Ne and ^{20}Mg from the isotopes of heavy nuclei with $Z = 82-102$ by analysing the decay half-lives. The energy released during the transitions, Q value, is given as

$$Q = \Delta M_{\rm p} - (\Delta M_{\rm c} + \Delta M_{\rm d}) + k(Z_{\rm p}^{\varepsilon} - Z_{\rm d}^{\varepsilon}), \qquad (14)$$

where $\Delta M_{\rm p}$, $\Delta M_{\rm d}$, $\Delta M_{\rm c}$ are the mass excess of the parent, daughter and the cluster, respectively. The term $k(Z_{\rm p}^{\varepsilon} - Z_{\rm d}^{\varepsilon})$ takes into account the screening effect of atomic electrons [79], where $k = 8.7$ eV, $\varepsilon = 2.517$ for $Z \geq 60$ and $k = 13.6$ eV, $\varepsilon = 2.408$ for $Z < 60$, derived using the data from [80]. To compute the Q value, the mass excess values are taken from Wang

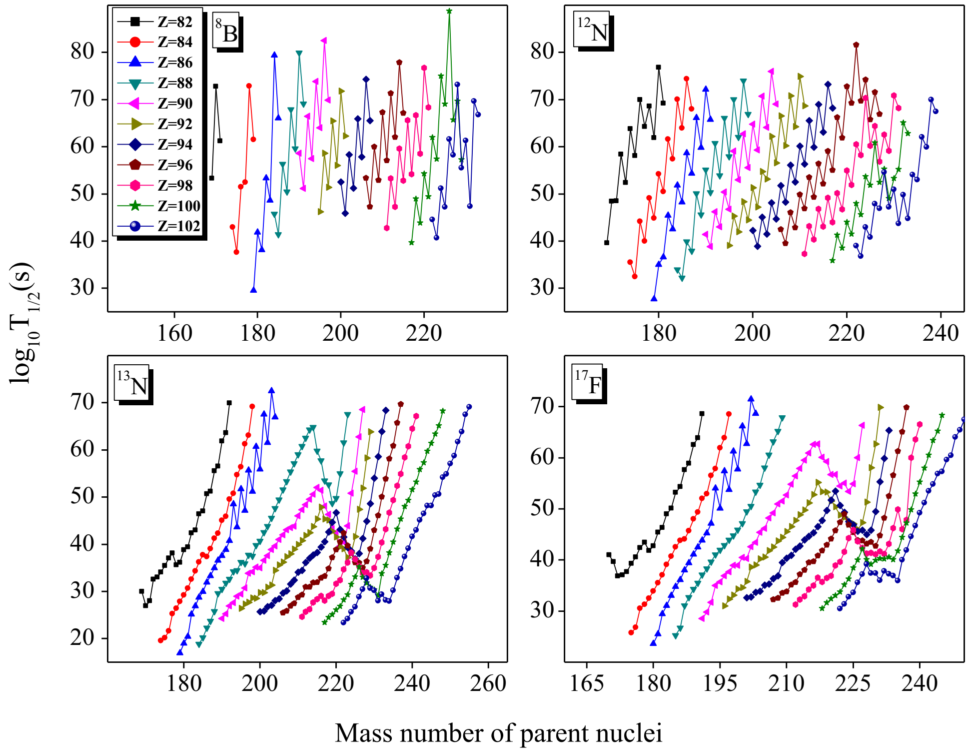

Figure 5. The computed $\log_{10} T_{1/2}$ values against mass number of the parent nuclei for the emission of 1p-halo nuclei from various isotopes of heavy nuclei, within the range $Z = 82-102$.

et al [77] and from the mass excess table of Koura *et al* [81]. The decay half-lives computed are for zero angular momentum transfers.

To check the possibility of emission of p-halo nucleus, we have estimated the decay half-lives. Generally, the radius of the nuclei R_i depends only on A_i, i.e. $R_i(A_i)$. Even if the surface effects are included through the Süsmann central radii C_i, still R_i is a function of A_i alone. Considering ^{8}B as a normal nucleus, we have calculated the radius using eq. (7) which is obtained as 2.2 fm and the Süsmann central radius is 1.745 fm. However, ^{8}B is a halo nucleus whose radius is found to be 2.38 fm, much larger than the value obtained by treating it as a normal nucleus. This implies that for a halo nucleus the radius is considerably larger than the normal nuclei and the radius of the halo nucleus does not follow the relation $R = R_0 A^{1/3}$. Also, the radius of the halo nucleus is observed to change from nucleus to nucleus and isotopes to isotopes. So, we have taken the matter radius of all the p-halo nuclei from [82].

Our theoretical estimations are shown in figures 5 and 6. We have included all the predictions except those for which the half-lives are above 10^{70} s, because in those cases the parent nucleus is considered to be highly stable against p-halo emissions. Figure 5 represents the theoretical predictions regarding the probability of 1p-halo emissions from heavy parents. Among the 1p-halo candidates, the HPR studies have shown that ^{8}B and ^{12}N could possibly be emitted from the ^{179}Rn heavy nucleus. The half-life suggests that the existence of these p-halos would be probable. It can be found that for ^{13}N emission from $^{169-171}$Pb isotopes, the predicted half-lives are 9.374×10^{29}, 9.243×10^{26} and 1.051×10^{28} s, respectively, which are well within the experimental upper limit ($T_{1/2} \leq 10^{30}$ s). Similar calculations are extended to other heavy nuclei ranging from $Z = 84$ to 102 and surprisingly, we have noticed that several isotopes of all heavy nuclei under consideration are unstable against ^{13}N halo emission, which implies the possibility of its emission from these parent nuclei. In the case of ^{17}F p-halo emission from $Z = 84-90$, 100, 102 heavy nuclei isotopes the half-life values obtained are within the experimental upper limit. The corresponding calculations for which half-lives are within the experimental limits are given in table 2. In figure 6, the emission of 2p-halo nuclei from various heavy parents has been displayed. The probability of emission of 2p-halo nuclei ^{9}C, ^{17}Ne, ^{18}Ne and ^{20}Mg from all available isotopes of heavy nuclei has been analysed extensively. Based on the theoretical half-lives prediction, it has been found that the 2p-halo ^{18}Ne could be emitted from a few isotopes of $Z = 84-88$, ^{190}Th and ^{195}U. When dealing with 2p-halo emission probability from heavy nuclei, its probability is observed to be less compared to 1p-halo nuclei, except for ^{18}Ne. In all these cases, the

Table 2. The predicted half-lives for the emission of different p-halo nuclei from various isotopes of heavy nuclei, within the range $82 \leq Z \leq 102$.

Parent nuclei	Emitted halo nuclei	Q value (MeV)	Penetrability, P	Decay constant, λ (s^{-1})	$\log_{10} T_{1/2}$ (s)
^{179}Rn	^{8}B	16.988	3.421×10^{-51}	1.795×10^{-30}	29.587
^{179}Rn	^{12}N	32.986	1.387×10^{-49}	1.275×10^{-28}	27.735
^{169}Pb	^{13}N	31.749	8.438×10^{-52}	7.393×10^{-31}	29.972
^{170}Pb	^{13}N	33.079	8.213×10^{-49}	7.497×10^{-28}	26.966
^{171}Pb	^{13}N	32.529	7.344×10^{-50}	6.593×10^{-29}	28.022
^{174}Po	^{13}N	38.082	1.730×10^{-41}	1.820×10^{-20}	19.581
^{175}Po	^{13}N	37.662	4.090×10^{-42}	4.250×10^{-21}	20.212
^{176}Po	^{13}N	36.842	1.730×10^{-43}	1.760×10^{-22}	21.595
^{177}Po	^{13}N	34.862	3.570×10^{-47}	3.440×10^{-26}	25.304
^{178}Po	^{13}N	34.262	2.840×10^{-48}	2.680×10^{-27}	26.412
^{179}Po	^{13}N	33.532	1.110×10^{-49}	1.030×10^{-28}	27.828
^{180}Po	^{13}N	32.830	4.460×10^{-51}	4.040×10^{-30}	29.234
^{181}Po	^{13}N	32.122	1.550×10^{-52}	1.380×10^{-31}	30.702
^{179}Rn	^{13}N	40.778	6.633×10^{-39}	7.465×10^{-18}	16.968
^{180}Rn	^{13}N	39.478	5.704×10^{-41}	6.214×10^{-20}	19.047
^{181}Rn	^{13}N	38.598	2.172×10^{-42}	2.314×10^{-21}	20.476
^{182}Rn	^{13}N	35.998	4.142×10^{-47}	4.115×10^{-26}	25.226
^{183}Rn	^{13}N	35.088	8.281×10^{-49}	8.019×10^{-28}	26.937
^{184}Rn	^{13}N	34.136	1.149×10^{-50}	1.082×10^{-29}	28.806
^{185}Rn	^{13}N	33.528	7.385×10^{-52}	6.833×10^{-31}	30.006
^{184}Ra	^{13}N	40.813	8.258×10^{-41}	9.302×10^{-20}	18.872
^{185}Ra	^{13}N	39.943	3.566×10^{-42}	3.931×10^{-21}	20.246
^{186}Ra	^{13}N	38.703	3.000×10^{-44}	3.204×10^{-23}	22.335
^{187}Ra	^{13}N	37.873	1.168×10^{-45}	1.221×10^{-24}	23.754
^{188}Ra	^{13}N	36.743	1.070×10^{-47}	1.085×10^{-26}	25.805
^{189}Ra	^{13}N	34.813	1.761×10^{-51}	1.692×10^{-30}	29.612
^{190}Ra	^{13}N	34.328	2.099×10^{-52}	1.989×10^{-31}	30.542
^{190}Th	^{13}N	38.808	3.243×10^{-46}	3.474×10^{-25}	24.300
^{191}Th	^{13}N	38.218	3.356×10^{-47}	3.539×10^{-26}	25.292
^{192}Th	^{13}N	37.298	7.549×10^{-49}	7.771×10^{-28}	26.950
^{193}Th	^{13}N	36.898	1.585×10^{-49}	1.614×10^{-28}	27.633
^{194}Th	^{13}N	36.168	6.971×10^{-51}	6.958×10^{-30}	28.998
^{195}Th	^{13}N	35.878	2.250×10^{-51}	2.228×10^{-30}	29.493
^{196}Th	^{13}N	35.228	1.258×10^{-52}	1.223×10^{-31}	30.753
^{195}U	^{13}N	38.782	2.605×10^{-48}	2.788×10^{-27}	26.395
^{196}U	^{13}N	38.232	3.020×10^{-49}	3.186×10^{-28}	27.337
^{197}U	^{13}N	38.002	1.387×10^{-49}	1.454×10^{-28}	27.678
^{198}U	^{13}N	37.462	1.552×10^{-50}	1.605×10^{-29}	28.635
^{199}U	^{13}N	37.452	1.869×10^{-50}	1.931×10^{-29}	28.555
^{200}U	^{13}N	36.812	1.238×10^{-51}	1.258×10^{-30}	29.741
^{201}U	^{13}N	36.742	1.117×10^{-51}	1.132×10^{-30}	29.787
^{202}U	^{13}N	36.142	8.177×10^{-53}	8.156×10^{-32}	30.929
^{200}Pu	^{13}N	40.217	1.092×10^{-47}	1.212×10^{-26}	25.757
^{201}Pu	^{13}N	40.107	8.751×10^{-48}	9.686×10^{-27}	25.855
^{202}Pu	^{13}N	39.527	9.422×10^{-49}	1.028×10^{-27}	26.829
^{203}Pu	^{13}N	39.347	5.470×10^{-49}	5.940×10^{-28}	27.067
^{204}Pu	^{13}N	38.747	4.992×10^{-50}	5.338×10^{-29}	28.113
^{205}Pu	^{13}N	38.527	2.353×10^{-50}	2.501×10^{-29}	28.443
^{206}Pu	^{13}N	37.827	1.245×10^{-51}	1.299×10^{-30}	29.727
^{207}Pu	^{13}N	37.567	4.676×10^{-52}	4.848×10^{-31}	30.155

Table 2. *Continued.*

Parent nuclei	Emitted halo nuclei	Q value (MeV)	Penetrability, P	Decay constant, λ (s^{-1})	$\log_{10} T_{1/2}$ (s)
^{206}Cm	^{13}N	41.412	2.034×10^{-47}	2.324×10^{-26}	25.474
^{207}Cm	^{13}N	41.142	8.427×10^{-48}	9.568×10^{-27}	25.860
^{208}Cm	^{13}N	40.472	6.393×10^{-49}	7.140×10^{-28}	26.987
^{209}Cm	^{13}N	40.172	2.227×10^{-49}	2.469×10^{-28}	27.448
^{210}Cm	^{13}N	39.422	1.069×10^{-50}	1.164×10^{-29}	28.775
^{211}Cm	^{13}N	39.082	2.946×10^{-51}	3.178×10^{-30}	29.339
^{212}Cm	^{13}N	38.202	6.773×10^{-53}	7.141×10^{-32}	30.987
^{211}Cf	^{13}N	42.987	1.340×10^{-46}	1.590×10^{-25}	24.639
^{212}Cf	^{13}N	42.317	1.143×10^{-47}	1.335×10^{-26}	25.715
^{213}Cf	^{13}N	41.957	3.288×10^{-48}	3.808×10^{-27}	26.260
^{214}Cf	^{13}N	41.117	1.236×10^{-49}	1.403×10^{-28}	27.694
^{215}Cf	^{13}N	40.677	2.355×10^{-50}	2.644×10^{-29}	28.418
^{216}Cf	^{13}N	40.267	4.949×10^{-51}	5.500×10^{-30}	29.100
^{217}Cf	^{13}N	40.737	4.655×10^{-50}	5.233×10^{-29}	28.122
^{218}Cf	^{13}N	40.197	5.534×10^{-51}	6.139×10^{-30}	29.053
^{219}Cf	^{13}N	39.917	1.984×10^{-51}	2.186×10^{-30}	29.501
^{217}Fm	^{13}N	44.742	2.019×10^{-45}	2.493×10^{-24}	23.444
^{218}Fm	^{13}N	44.062	1.815×10^{-46}	2.207×10^{-25}	24.497
^{219}Fm	^{13}N	43.632	4.150×10^{-47}	4.997×10^{-26}	25.142
^{220}Fm	^{13}N	43.022	4.469×10^{-48}	5.307×10^{-27}	26.116
^{221}Fm	^{13}N	42.562	8.466×10^{-49}	9.944×10^{-28}	26.843
^{222}Fm	^{13}N	41.722	3.149×10^{-50}	3.626×10^{-29}	28.281
^{223}Fm	^{13}N	41.122	2.982×10^{-51}	3.385×10^{-30}	29.311
^{222}No	^{13}N	45.897	2.019×10^{-45}	2.493×10^{-24}	23.380
^{223}No	^{13}N	45.327	1.815×10^{-46}	2.207×10^{-25}	24.230
^{224}No	^{13}N	44.417	1.178×10^{-47}	1.444×10^{-26}	25.681
^{225}No	^{13}N	43.787	1.186×10^{-48}	1.433×10^{-27}	26.684
^{226}No	^{13}N	42.537	8.641×10^{-51}	1.014×10^{-29}	28.835
^{227}No	^{13}N	41.607	2.025×10^{-52}	2.326×10^{-31}	30.474
^{228}No	^{13}N	40.337	9.030×10^{-55}	1.005×10^{-33}	32.838
^{229}No	^{13}N	41.407	1.268×10^{-52}	1.449×10^{-31}	30.680
^{230}No	^{13}N	41.607	3.674×10^{-52}	4.219×10^{-31}	30.216
^{231}No	^{13}N	42.767	6.109×10^{-50}	7.211×10^{-29}	27.983
^{232}No	^{13}N	41.977	2.647×10^{-51}	3.066×10^{-30}	29.354
^{233}No	^{13}N	42.587	4.216×10^{-50}	4.955×10^{-29}	28.146
^{234}No	^{13}N	42.657	6.808×10^{-50}	8.014×10^{-29}	27.937
^{235}No	^{13}N	41.397	3.786×10^{-52}	4.325×10^{-31}	30.205
^{174}Po	^{17}F	51.169	9.309×10^{-48}	1.295×10^{-26}	25.728
^{175}Po	^{17}F	50.419	7.827×10^{-49}	1.073×10^{-27}	26.810
^{176}Po	^{17}F	48.169	1.552×10^{-52}	2.033×10^{-31}	30.533
^{179}Rn	^{17}F	54.045	9.812×10^{-46}	1.442×10^{-24}	23.682
^{180}Rn	^{17}F	52.775	1.401×10^{-47}	2.009×10^{-26}	25.538
^{181}Rn	^{17}F	50.305	1.648×10^{-51}	2.254×10^{-30}	29.488
^{184}Ra	^{17}F	54.620	2.431×10^{-47}	3.609×10^{-26}	25.283
^{185}Ra	^{17}F	53.620	9.058×10^{-49}	1.320×10^{-27}	26.720
^{190}Th	^{17}F	54.046	1.303×10^{-50}	1.914×10^{-29}	28.559
^{191}Th	^{17}F	53.176	6.890×10^{-52}	9.960×10^{-31}	29.842
^{217}Fm	^{17}F	60.317	1.185×10^{-52}	1.943×10^{-31}	30.552
^{222}No	^{17}F	61.903	1.420×10^{-52}	2.390×10^{-31}	30.463
^{174}Po	^{18}Ne	56.948	2.796×10^{-47}	4.324×10^{-26}	25.205
^{175}Po	^{18}Ne	54.838	1.315×10^{-50}	1.958×10^{-29}	28.549

Table 2. *Continued.*

Parent nuclei	Emitted halo nuclei	Q value (MeV)	Penetrability, P	Decay constant, λ (s^{-1})	$\log_{10} T_{1/2}$ (s)
^{176}Po	^{18}Ne	53.778	2.947×10^{-52}	4.304×10^{-31}	30.207
^{179}Rn	^{18}Ne	58.335	6.248×10^{-48}	9.897×10^{-27}	25.845
^{180}Rn	^{18}Ne	57.115	9.651×10^{-50}	1.497×10^{-28}	27.666
^{181}Rn	^{18}Ne	55.805	9.162×10^{-52}	1.388×10^{-30}	29.698
^{184}Ra	^{18}Ne	59.121	1.582×10^{-49}	2.540×10^{-28}	27.436
^{185}Ra	^{18}Ne	57.821	1.761×10^{-51}	2.764×10^{-30}	29.399
^{186}Ra	^{18}Ne	56.821	6.247×10^{-41}	1.094×10^{-19}	30.915
^{190}Th	^{18}Ne	58.788	9.184×10^{-53}	1.466×10^{-31}	30.675
^{195}U	^{18}Ne	61.334	1.891×10^{-51}	3.149×10^{-30}	29.343

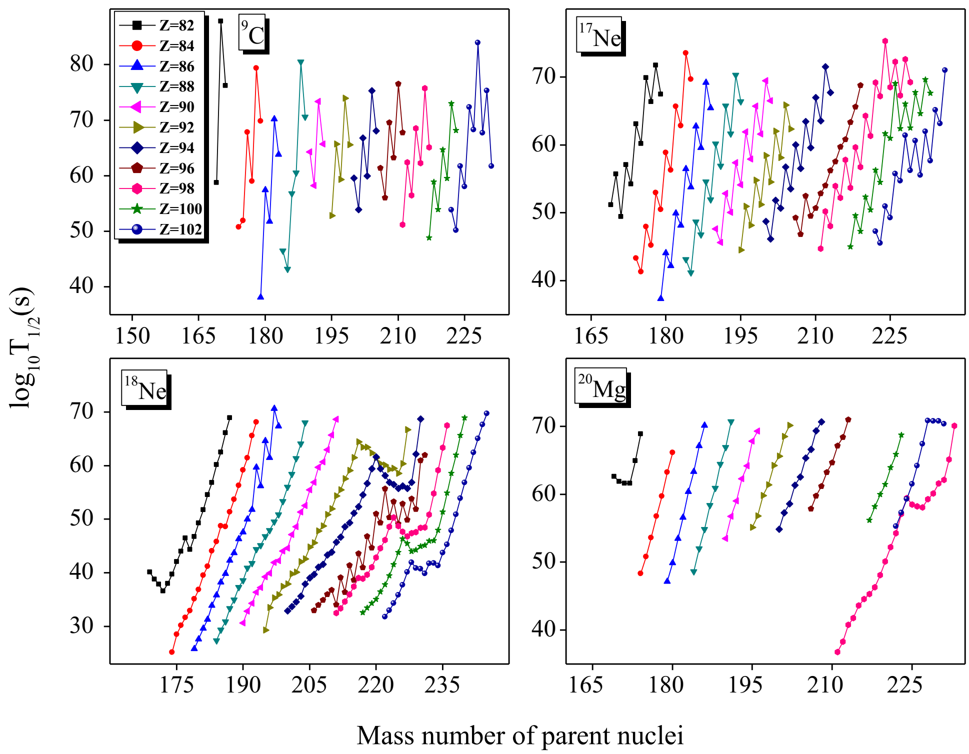

Figure 6. The computed $\log_{10} T_{1/2}$ values against mass number of the parent nuclei for the emission of 2p-halo nuclei from various isotopes of heavy nuclei, within the range $Z = 82-102$.

half-lives that are well inside the experimental upper limit are listed in table 2.

Further, to compare the probability of emission of a halo nucleus with that of the normal cluster emission, we have treated ^{13}N as a halo nucleus and also treated it as a normal cluster and studied the probability of emission via HPR. We have calculated the half-lives of ^{13}N emission from parents with Z values 82, 86, 90, 92, 94, 98, 100 and 102, randomly chosen. As the emitted halo is considered as a normal cluster, the matter radius, $R_i = R_i(A_i)$, unlike halo, is obtained using eq. (7). It is observed that the penetrability gets increased and accordingly, the half-lives are lowered. For example, consider the p-halo, ^{13}N, emitted from the parent nucleus ^{169}Pb. When the emitted halo is considered as a normal cluster, the half-life predicted is 8.255×10^{25} s and in the other case, when it is considered as a p-halo, the half-life is 9.374×10^{29} s, i.e. it is raised by an order of four. A plot of $\log_{10} T_{1/2}$ vs. mass number of the parent nuclei for p-halo emission and for normal cluster emission are shown in figures 7 and 8, respectively. A result of the present comparison study, shown in figures 7 and 8, is that the chance of emitting a p-halo nucleus from heavy parent nuclei is less compared to that of its emission when treated as a normal cluster. However, remarkably, there are finite possibilities of p-halo emissions from heavy nuclei, which are strongly demonstrated by our predictions using CPPM.

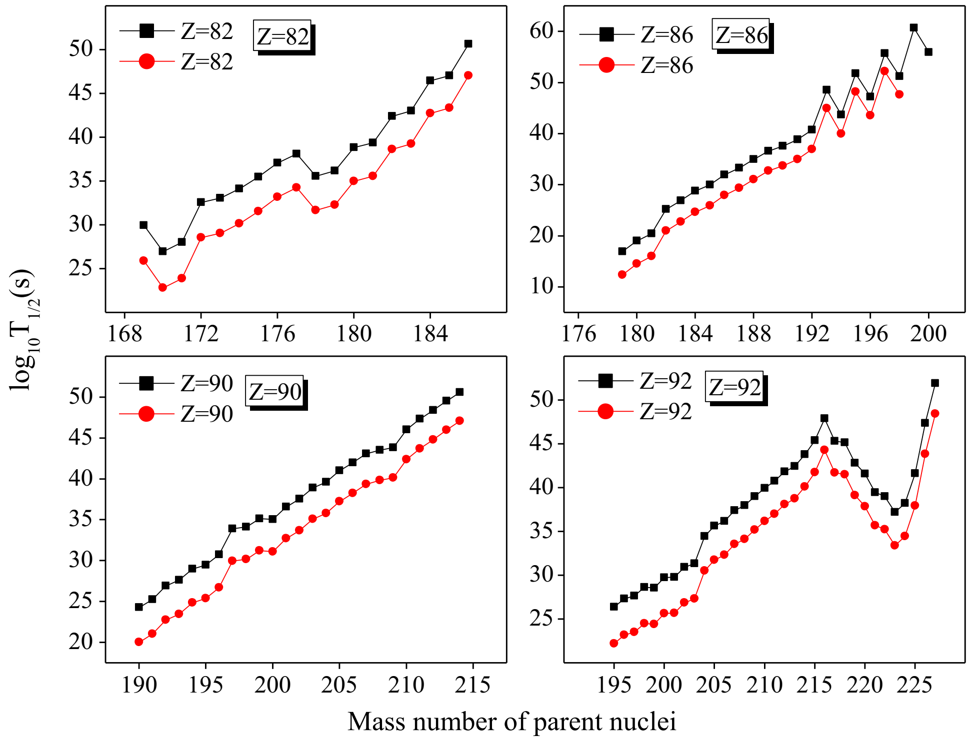

Figure 7. Comparison of the predicted heavy particle decay half-lives of the cluster and the p-halo, ^{13}N, for parent nuclei with $Z = 82, 86, 90, 92$.

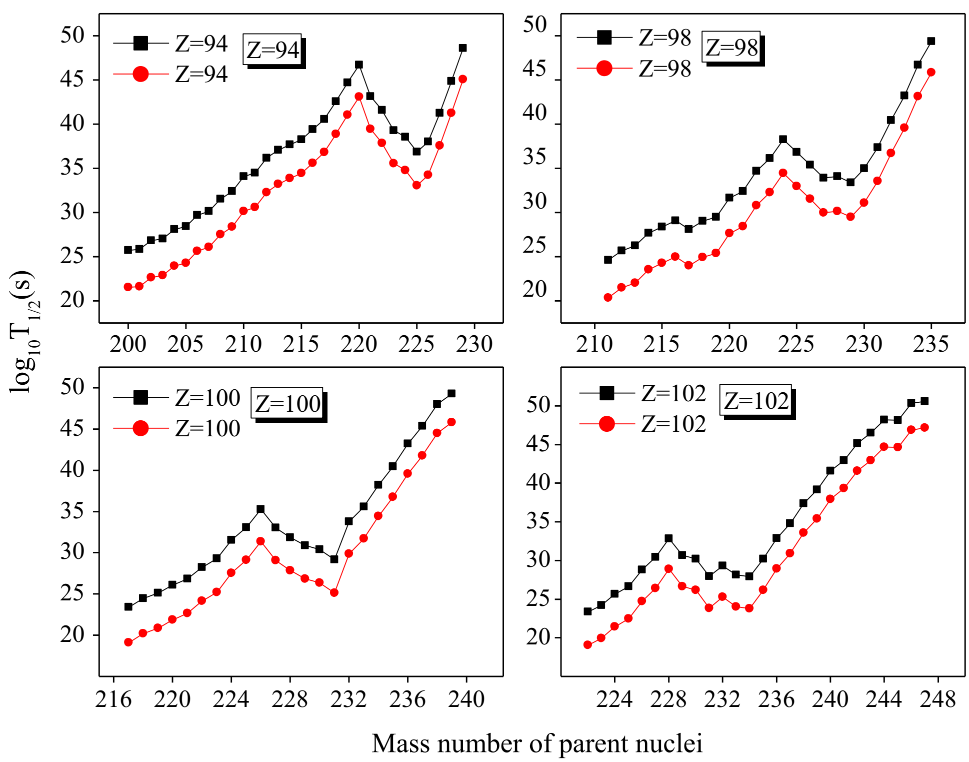

Figure 8. Comparison of the predicted heavy particle decay half-lives of the cluster and the p-halo,^{13}N, for parent nuclei with $Z = 94, 98, 100, 102$.

4. Conclusion

In summary, we have studied the p-halo structure of a nucleus based on separation energy consideration and potential energy calculations. The probable p-halo emissions from various isotopes of heavy nuclei, $Z = 82-102$, have been analysed by evaluating decay half-lives for the emission of p-halos ^{8}B, ^{9}C, ^{12}N, ^{13}N, ^{17}F, ^{17}Ne, ^{18}Ne and ^{20}Mg. The plot $\log_{10} T_{1/2}$ (s) against mass number of the parent nuclei for all the p-halo emissions displayed the entire calculations. The obtained half-lives for p-halo nuclei that are within the present experimental upper limit, $T_{1/2}$ (s) $\leq 10^{30}$ (s), are listed in table 2. The nuclei ^{8}B, ^{12}N, ^{13}N, ^{17}F and ^{18}Ne are found to be the probable p-halo nuclei that could be emitted from various heavy nuclei. In addition, the HPR study performed by considering halo nuclei as a normal cluster indicated that the halo particle emissions from heavy nuclei are less probable compared to normal cluster emissions, but still the probability that a p-halo could be emitted from heavy nuclei is finite. The study will be helpful for understanding the existence of halo states in proton dripline.

References

[1] P G Hansen and A S Jensen, *Annu. Rev. Nucl. Part. Sci.* **45**, 591 (1995)
[2] J Al-Khalili, *Lect. Notes Phys.* **651**, 77 (2004)
[3] G Saxena and D J Singh, *Exp. Theor. Phys.* **116**, 567 (2013)
[4] R J Carroll, R D Page, D T Joss, J Uusitalo, I G Darby, K Andgren, B Cederwall, S Eeckhaudt, T Grahn, C Gray-Jones, P Greenlees, B Hadinia, P Jones, R Julin, S Juutinen, M Leino, A P Leppänen, M Nyman, D O Donnell, J Pakarinen, P Rahkila, M Sandzelius, J Sarén, C Scholey, D Seweryniak and J B Simpson, *Phys. Rev. Lett.* **12**, 092501 (2014)
[5] I Tanihata, H Hamagaki, O Hashimoto, Y Shida, N Yoshikawa, K Sugimoto, O Yamakawa, T Kobayashi and N Takahashi, *Phys. Rev. Lett.* **55**, 2676 (1985)
[6] I Tanihata, H Hamagaki, O Hashimoto, S Nagamiya, Y Shida, N Yoshikawa, O Yamakawa, K Sugimoto, T Kobayashi, D E Greiner, N Takahashi and Y Nojiri, *Phys. Lett. B* **160**, 380 (1985)
[7] P G Hansen and B Jonson, *Europhys. News* **4**, 409 (1987)
[8] S Bottoni *et al*, *Phys. Rev. C* **92**, 024322 (2015)
[9] N Kobayashi *et al*, *Phys. Rev. C* **86**, 054604 (2012)
[10] I Tanihata *et al*, *Phys. Rev. Lett.* **100**, 192502 (2008)
[11] S E A Orrigo and H Lenske, *Phys. Lett. B* **677**, 214 (2009)
[12] T Bjerge and K J Borgstrom, *Nature* **138**, 400 (1936)
[13] R Kanungo *et al*, *Phys. Rev. Lett*. **117**, 102501 (2016)
[14] A Estrade *et al*, *Phys. Rev. Lett.* **113**, 132501 (2014)
[15] K Tanaka *et al*, *Phys. Rev. Lett.* **104**, 062701 (2010)
[16] Y Togano *et al*, *Phys. Lett. B* **761**, 412 (2016)
[17] M Takechi *et al*, *Phys. Rev. C* **90**, 061305 (2014)
[18] N Kobayashi *et al*, *Phys. Rev. Lett.* **112**, 242501 (2014)
[19] K E Rehm *et al*, *Phys. Rev. Lett.* **81**, 3341 (1998)
[20] A D Pietro, V Scuderi, A M Moro, L Acosta, F Amorini, M J G Borge, P Figuera, M Fisichella, L M Fraile and J G Camacho, *Phys. Rev. C* **85**, 054607 (2012)
[21] M Mazzocco, C Signorini, M Romoli, A D Franesco, M DiPietro, E Vardaci, K Yoshida, R Yoshida, A Bonetti, A DeRosa and T Glodariu, *Eur. Phys. J. A* **28**, 295 (2006)
[22] V Morcelle *et al*, *Phys. Lett. B* **732**, 228 (2014)
[23] O R Kakuee *et al*, *Nucl. Phys. A* **728**, 339 (2003)
[24] A M S Benıtez *et al*, *Nucl. Phys. A* **803**, 30 (2008)
[25] L Acosta *et al*, *Phys. Rev. C* **84**, 044604 (2011)
[26] L Standyło *et al*, *Phys. Rev. C* **87**, 064603 (2013)
[27] R Wolski *et al*, *Eur. J. Phys. A* **47**, 111 (2011)
[28] M Cubero *et al*, *Phys. Rev. Lett.* **109**, 262701 (2012)
[29] J Casal, M Gómez-Ramos and A M Moro, *Phys. Lett. B* **767**, 307 (2017)
[30] H Simon, D Aleksandrov, T Aumann, L Axelsson, T Baumann, M J G Borge, L V Chulkov, R Collatz, J Cub, W Dostal, B Eberlein, T W Elze, H Emling, H Geissel, A Grünschloss, M Hellström, J Holeczek, R Holzmann, B Jonson, J V Kratz, G A Kraus, R Kulessa, Y Leifels, A Leistenschneider, T Leth, I Mukha, G Münzenberg, F Nickel, T Nilsson, G Nyman, B Petersen, M Pfützner, A Richter, K Riisager, C Scheidenberger, G Schrieder, W Schwab, M H Smedberg, J Stroth, Surowiec, O Tengblad and M V Zhukov, *Phys. Rev. Lett.* **83**, 496 (1999)
[31] M Aygun, *Pramana – J. Phys.* **88**: 53 (2017)
[32] N Keeley, K W Kemper and K Rusek, *Eur. Phys. J. A* **50**, 145 (2014)
[33] K Whitmore, D Smalley, H Iwasaki, T Suzuki, V M Bader, D Bazin, J S Berryman, B A Brown, C M Campbell, P Fallon, A Gade, C Langer, A Lemasson, C Loelius, A O Macchiavelli, C Morse, T Otsuka, J Parker, F Recchia, S R Stroberg, D Weisshaar and K Wimmer, *Phys. Rev. C* **91**, 041303(R) (2015)
[34] T Aumann, *Eur. Phys. J. A* **26**, 441 (2005)
[35] M V Zhukov, B V Danilin, D V Fedorov, J M Bang, I J Thompson and J S Vaagen, *Phys. Rep.* **231**, 151 (1993)
[36] S C Pieper and R B Wiringa, *Annu. Rev. Nucl. Part. Sci.* **51**, 53 (2001)
[37] D J Dean and M H Jensen, *Rev. Mod. Phys.* **75**, 607 (2003)
[38] M K Sharma, R N Panda, M K Sharma and S K Patra, *Phys. Rev. C* **93**, 014322 (2016)
[39] M Kamimura, M Yahiro, Y Iseri, Y Sakuragi, H Kameyama and M Kawai, *Prog. Theor. Phys. Suppl.* **89**, 1 (1986)
[40] A Ono, H Horiuchi, T Maruyama and A Ohnishi, *Phys. Rev. Lett.* **68**, 2898 (1992)
[41] V Varga, Y Suzuki and R G Lovas, *Nucl. Phys. A* **571**, 447 (1994)

[42] Y Kucuk and E Aciksoz, *Eur. Phys. J. A* **52**, 98 (2016)
[43] M V Zhukov and I J Thompson, *Phys. Rev. C* **52**, 6 (1995)
[44] T Minamisono, T Ohtsubo, I Minami, S Fukuda, A Kitagawa, M Fukuda, K Matsuta, Y Nojiri, S Takeda, H Sagawa and H Kitagawa, *Phys. Rev. Lett.* **69**, R14 (1992)
[45] R K Gupta, S Kumar, M Balasubramaniam, G Munzenberg and W Scheid, *J. Phys. G: Nucl. Part. Phys.* **28**, 699 (2002)
[46] R K Biju, M K Preethi Rajan and K P Santhosh, *Proceedings of the DAE- Symposium on Nuclear Physics,* edited by B K Nayak, D Dutta and S M Sharma (Prudent Art & Fab Pvt Ltd, India, 2015) Vol. 60, p. 152
[47] G Sawhney, M K Sharma and R K Gupta, *J. Phys. G: Nucl. Part. Phys.* **41**, 055101 (2014)
[48] S Watanabe, K Minomo, M Shimada, S Tagami, M Kimura, M Takechi, M Fukuda, D Nishimura, T Suzuki, T Matsumoto, Y R Shimizu and M Yahiro, *Phys. Rev. C* **89**, 044610 (2014)
[49] W Schwab *et al*, *Z. Phys. A* **350**, 283 (1995)
[50] V Guimarães, J J Kolata, D Peterson, P Santi, R H W Stevens, S M Vincent, F D Becchetti, M Y Lee, T W Odonnell, D A Roberts and J A Zimmerman, *Phys. Rev. Lett* **84**, 1862 (2000)
[51] A Ozawa, T Kobayashi, H Sato, D Hirata, I Tanihata, O Yamakawa, K Omata, K Sugimoto, D Olson, W Christie and H Wieman, *Phys. Lett. B* **334**, 18 (1994)
[52] D Q Fang *et al*, *Phys. Rev. C* **76**, 031601 (2007)
[53] R Morlock, R Kunz, A Mayer, M Jaeger, A Müller and J W Hammer, *Phys. Rev. Lett.* **79**, 3837 (1997)
[54] Z Ren, B Chen, Z Ma and G Xu, *Phys. Rev. C* **53**, R572, (1996)
[55] X Z Cai *et al*, *Phys. Rev. C* **65**, 024610 (2002)
[56] E F Aguilera, P A Valenzuela, E M Quiroz and J F Arnaiz, J J Kolata and V Guimaraes, *Phys. Rev. C* **93**, 034613 (2016)
[57] J Lubian, T Correa, E F Aguilera, L F Canto, A G Camacho, E M Quiroz and P R S Gomes, *Phys. Rev. C* **79**, 064605 (2009)
[58] J A Tostevin, F M Nunes and I J Thompson, *Phys. Rev. C* **63**, 024617 (2001)
[59] A Pakou *et al*, *Phys. Rev. C* **87**, 014619 (2013)
[60] A Barioni, J C Zamora, V Guimaraes, B Paes, J Lubian, E F Aguilera, J J Kolata, A L Roberts, F D Becchetti, A Villano, M Ojaruega and H Jiang, *Phys. Rev. C* **84**, 014603 (2011)
[61] J Rangel, J Lubian, P R S Gomes, B V Carlson, L C Chamon and A Gomez-Camacho, *Eur. Phys. J. A* **49**, 57 (2013)
[62] J Rangel, J Lubian, L F Canto and P R S Gomes, *Phys. Rev. C* **93**, 054610 (2016)
[63] L F Canto, P R S Gomes, R Donangelo and M S Hussein, *Phys. Rep.* **424**, 1 (2006)
[64] A Sandulescu, D N Poenaru and W Greiner, *Sovt. J. Part. Nucl.* **11**, 528 (1980)
[65] H J Rose and G A Jones, *Nature* **307**, 245 (1984)
[66] K P Santhosh and B Priyanka, *Phys. Rev. C* **87**, 064611 (2013)
[67] K P Santhosh and B Priyanka, *Int. J. Mod. Phys. E* **22**, 11 (2013)
[68] K P Santhosh and B Priyanka, *Eur. Phys. J. A* **49**, 66 (2013)
[69] K P Santhosh and B Priyanka, *Int. J. Mod. Phys. E* **23**, 1450059 (2014)
[70] K P Santhosh and A Joseph, *Pramana – J. Phys.* **55**, 375 (2000)
[71] K P Santhosh and A Joseph, *Pramana – J. Phys.* **58**, 611 (2002)
[72] Y J Shi and W J Swiatecki, *Phys. Rev. Lett.* **54**, 300 (1985)
[73] J Blocki, J Randrup, W J Swiatecki and C F Tsang, *Ann. Phys. (NY)* **105**, 427 (1977)
[74] J Blocki and W J Swiatecki, *Ann. Phys. (NY)* **132**, 53 (1981)
[75] D N Poenaru, M Ivascu, A Sandulescu and W Greiner, *J. Phys. G* **10**, L183 (1984)
[76] S Athanassopoulos, E Mavrommatis, K A Gernoth and J W Clark, arXiv: nucl-th/0509075v1 (2005)
[77] M Wang, G Audi, A H Wapstra, F G Kondev, M MacCormick, X Xu and B Pfeiffer, *Chin. Phys. C* **36**, 1603 (2012)
[78] A Leistenschneider *et al*, *Phys. Rev. Lett.* **86**, 5442 (2001)
[79] V Yu Denisov and H Ikezoe, *Phys. Rev. C* **72**, 064613 (2005)
[80] K N Huang, M Aoyagi, M H Chen, B Crasemann and H Mark, *At. Data Nucl. Data Tables* **18**, 243 (1976)
[81] H Koura, T Tachibana, M Uno and M Yamada, *Prog. Theor. Phys.* **113**, 305 (2005)
[82] A Ozawa, T Suzuki and I Tanihata, *Nucl. Phys. A* **693**, 32 (2001)